

Effects of Crowding and Environment on the Evolution of Conformational Ensembles of the Multi-Stimuli-Responsive Intrinsically Disordered Protein, Rec1-Resilin: A Small-Angle Scattering Investigation

Rajkamal Balu,[‡] Jitendra P. Mata,[§] Robert Knott,[§] Christopher M. Elvin,^{||} Anita J. Hill,[⊥] Namita R. Choudhury,^{†,‡} and Naba K. Dutta^{*,†,‡}

[†]School of Chemical Engineering, The University of Adelaide, Adelaide, SA 5005, Australia

[‡]Future Industries Institute, University of South Australia, Mawson Lakes, SA 5095, Australia

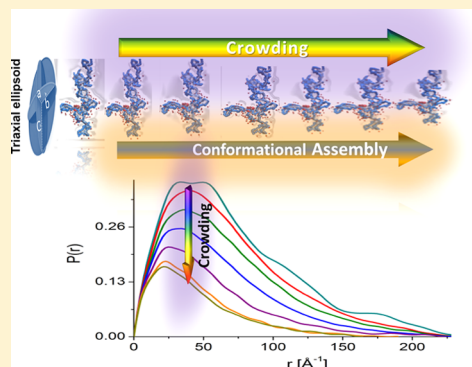
[§]Bragg Institute, ANSTO, Private Mail Bag, Kirrawee, NSW 2232, Australia

^{||}CSIRO Agriculture, Level 6, Queensland Bioscience Precinct, St Lucia, QLD 4067, Australia

[⊥]CSIRO Manufacturing, Bayview Avenue, Clayton, VIC 3168, Australia

Supporting Information

ABSTRACT: In this study, we explore the overall structural ensembles and transitions of a biomimetic, multi-stimuli-responsive, intrinsically disordered protein (IDP), Rec1-resilin. The structural transition of Rec1-resilin with change in molecular crowding and environment is evaluated using small-angle neutron scattering and small-angle X-ray scattering. The quantitative analyses of the experimental scattering data using a combination of computational models allowed comprehensive description of the structural evolution, organization, and conformational ensembles of Rec1-resilin in response to the changes in concentration, pH, and temperature. Rec1-resilin in uncrowded solutions demonstrates the equilibrium intrinsic structure quality of an IDP with radius of gyration $R_g \sim 5$ nm, and a scattering function for the triaxial ellipsoidal model best fit the experimental dataset. On crowding (increase in concentration >10 wt %), Rec1-resilin molecules exert intermolecular repulsive force of interaction, the R_g value reduces with a progressive increase in concentration, and molecular chains transform from a Gaussian coil to a fully swollen coil. It is also revealed that the structural organization of Rec1-resilin dynamically transforms from a rod (pH 2) to coil (pH 4.8) and to globular (pH 12) as a function of pH. The findings further support the temperature-triggered dual-phase-transition behavior of Rec1-resilin, exhibiting rod-shaped structural organization below the upper critical solution temperature (~ 4 °C) and a large but compact structure above the lower critical solution temperature (~ 75 °C). This work attempted to correlate unusual responsiveness of Rec1-resilin to the evolution of conformational ensembles.



1. INTRODUCTION

Native resilin, a member of the family of elastic proteins (that includes elastin, abductin, collagen, gluten, spider silks, byssus, and titin), is currently considered as the most resilient (~97%) biomaterial known.¹ Native resilin is a di- and trityrosine-cross-linked extra-cellular matrix protein with a fatigue life in excess of 300 million cycles, and it plays a major role in the jumping, flying, and sound production mechanisms in many arthropods.¹ The resilin gene sequence of the fruit fly *Drosophila melanogaster* was first identified by Ardell et al.² in 2001 that unlocked the potential for biosynthesis of resilin-mimetic proteins (RMPs). In 2005, Elvin et al.¹ reported the cloning, expression, and photo-cross-linking of the first RMP, Rec1-resilin. Since then, a variety of RMPs and resilin-like-polypeptides with exquisite control over the amino acid sequence comprising repeat resilin motifs have been success-

fully designed and synthesized and have been the subject of significant research interest and excitement.^{3–5} Over the past decade, RMPs with precise structural motifs have evolved as a class of multi-stimuli-responsive advanced material with significant promise in the areas of biotechnology, medicine, and nanotechnology. Extensive research has been conducted by Dutta and co-workers to explore the unusual environmental responsiveness of Rec1-resilin⁶ and its potential use in creating patterned surfaces,⁷ responsive interfaces,⁸ and multifunctional soft templates to develop designer (size- and shape-controlled) nano- and sub-nanoparticles with unique photophysical and electrochemical characteristics.^{9–12} The cross-linked swollen

Received: March 9, 2016

Revised: June 7, 2016

Published: June 9, 2016



hydrogels of Rec1-resilin also demonstrate outstanding rubber-like elasticity, unusual resilience (>94%), and creep resistance behavior.^{1,13} Most recently, we have also reported the structural details of Rec1-resilin in dilute aqueous solutions and confirmed it to be an intrinsically disordered protein (IDP), a class of biologically active proteins that lacks defined tertiary and often secondary structures.¹⁴ However, being an IDP, a limited number of experimental techniques are suited for investigations to decipher its molecular mode of action and assembly at a structural level; hence, they still remain highly challenging. An IDP in general displays broad ensembles of rapidly interconverting conformations. Consequently, the individual conformation is not easily illustrated by simple parameters, and the nature of ensembles also remains controversial. In spite of the lack of a well-defined structure, in the conventional sense, it has been clearly identified that IDPs fulfill essential functions in eukaryotic life and therefore challenge the conventional protein structure–function paradigm.^{15,16} They have now been recognized as intriguing substrates for intense examination in modern proteomics and have revolutionized structural biology in recent years.^{17,18}

Proteins in an aqueous solution are known to interact through various types of protein–protein and protein–water (both inter- and intramolecular) forces that ultimately control the conformational ensembles and characteristics of proteins including protein solubility and stability. The change in protein concentration may have a dramatic effect on the conformational ensembles and their organization, morphology, and function. Kato et al.¹⁹ have recently presented compelling evidence that low-complexity protein sequences/random coil polypeptides can undergo a concentration-dependent transformation to extended β -sheet aggregates at higher concentrations. Vondel et al.²⁰ have demonstrated that the local structure in proteins changes significantly with crowding and the effect depends on the employed crowding agent and its concentration.

One of the intriguing questions remaining unanswered to date is how the secondary structure of multi-stimuli-responsive RMPs evolves with environment (including pH, temperature, and concentration, i.e., changes from a dilute to a dense state). Such information is critical to understand the molecular origin of multiresponsiveness, outstanding elasticity, resilience, and fatigue characteristics of native resilin gels and responsive hydrogels of RMPs. In pursuit of this question, herein, we investigate and report the first study of the evolution of the secondary structure and morphology of Rec1-resilin from dilute to concentrated aqueous solutions and with change in environmental conditions using small-angle scattering (SAS), both small-angle X-ray scattering (SAXS) and small-angle neutron scattering (SANS) techniques.

SAS is of great importance for the determination of the structure–property relationship of IDPs such as Rec1-resilin that cannot be successfully crystallized.^{21,22} SAXS and SANS are the two complementary techniques that have been used to evaluate the molecular structure, shape, self-assembly, particle–particle interaction, and organization of complex biological systems close to physiological conditions.^{22,23} SAS has been widely used to investigate the solvation properties of proteins,²⁴ as well as understanding protein interactions in solutions.^{25–28} SAXS can generally provide good structural images of proteins in dilute solutions as X-rays interact most efficiently with electron-rich atoms such as nitrogen and oxygen.²⁹ On the other hand, SANS is particularly advantageous in studying the aggregation behavior of macromolecules in concentrated

solution phases because of sensitivity of neutrons to light elements such as hydrogen.^{30,31} The use of both of the techniques simultaneously enables us to identify the structural details of disordered systems over a wide range of concentrations. SANS and SAXS also provide complementary information due to the different responses to the hydration shell surrounding proteins and can be used for describing structural rearrangements of complex disordered proteins.³² Use of deuterated water (D_2O) instead of H_2O in SANS measurements provides a valuable contrast, which is sometimes difficult to achieve in SAXS.

2. EXPERIMENTAL SECTION

2.1. Synthesis and Purification of Rec1-Resilin. A synthetic Rec1-resilin construct (exon-1 of *D. melanogaster* resilin) was expressed and purified using a recombinant cloning protocol as reported by Elvin et al.³² (section S1 in Supporting Information). The protein polymer consisting of 310 amino acid residues with 18 copies of a 15-residue repeat consensus sequence, GGRPSDSYGYAPGGGN (Figure S1A), was verified to be pure with a molecular mass of 28.5 kDa, measured using matrix-assisted laser desorption ionization time-of-flight mass spectroscopy (Figure S1B). Rec1-resilin solutions of required concentration were prepared in phosphate-buffered saline (PBS) unless otherwise indicated. In the case of SANS measurement, D_2O was used instead of water to minimize incoherent scattering.

2.2. Dynamic Light Scattering. A computer-controlled Zetasizer Nano ZS (Malvern Instruments, Malvern, U.K.) was used for dynamic light scattering measurements on Rec1-resilin samples and to calculate the hydrodynamic diameter, D_h .

2.3. SAXS Experiment and Analysis. For SAXS analysis, Rec1-resilin was dissolved in 10 mM PBS, prepared using Milli-Q Gradient A10 purified water. The samples were placed in 2 mm i.d. quartz microcapillaries and analyzed as a function of concentration (1, 5, 10, 15, 20, 25, and 30 wt % at 25 °C; pH 7.4), pH (2, 4.8, 7.4, and 12 pH at 25 °C; 10 wt %), and temperature (4, 25, and 75 °C at pH 7.4; 5 wt %). SAXS measurements were performed using a NanoSTAR II SAXS instrument (Bruker AXS, Karlsruhe) with Cu K α radiation ($\lambda = 1.54 \text{ \AA}$). A scattering vector, q (eq 1), in the range of 0.012–0.39 \AA^{-1} was used for the measurements.²¹

$$q = \frac{4\pi \sin \theta}{\lambda} \quad (1)$$

where θ is the angle of scattering and λ is the wavelength of the X-rays. In all cases, the instrument and buffer backgrounds were subtracted from the sample signal to obtain the corrected intensity. The structural parameters of Rec1-resilin were determined from SAXS data fits using the “PRIMUS” program.³³

2.4. SANS Experiment and Analysis. For SANS analysis, Rec1-resilin was dissolved in 10 mM PBS, prepared using D_2O . The samples were placed in Hellma cells of path length 2 mm for analysis. The samples were analyzed as a function of concentration (1, 3, 5, 7, and 10 wt % at 25 °C; pH 7.4), pH (2, 4.8, 7.4, and 12 pH at 25 °C; 10 wt %), and temperature (4, 25, and 75 °C at pH 7.4; 5 wt %) using the Quokka SANS instrument at OPAL, Australian Nuclear Science and Technology Organization (ANSTO), Sydney, with neutrons (5 \AA) focused from a large liquid- D_2O cold source. Source aperture to sample aperture distances of 2, 8, and 20 m were employed to cover the scattering vector, q (eq 1), in the range

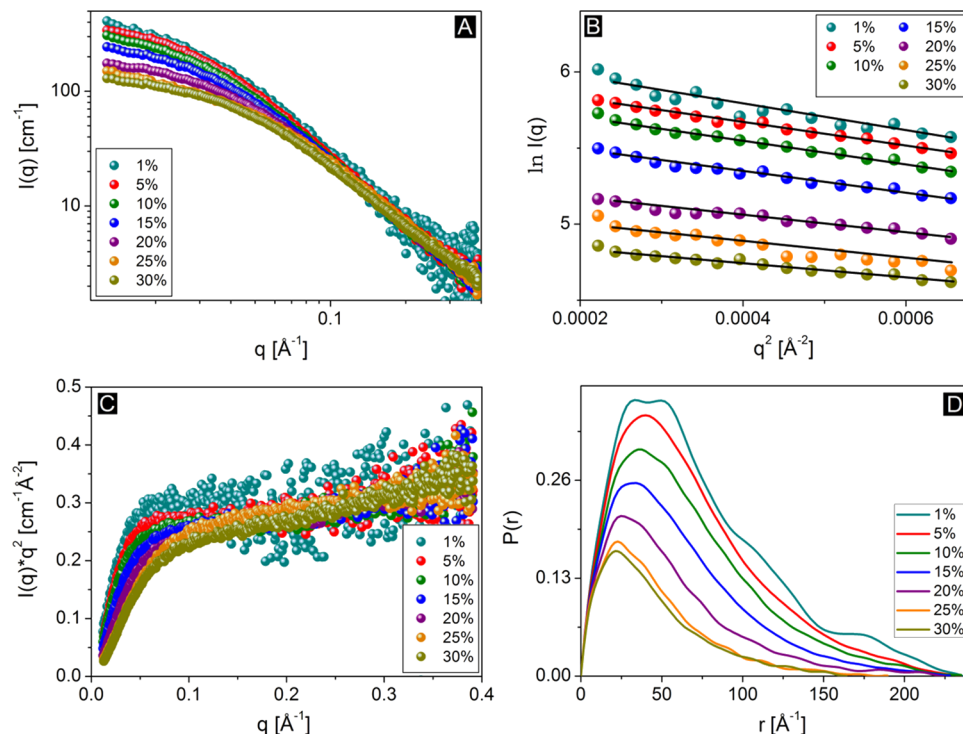


Figure 1. (A) Concentration-normalized SAXS intensity profile, $I(q)/(I_0/C_p)$, over a wide range of concentration, (B) corresponding Guinier approximation, where R_g is calculated from the slope of the straight line, (C) Kratky plot of the protein solutions, and (D) pair-distance distribution function of Rec1-resilin solutions as a function of concentration at pH 7.4 and 25 °C.

of $0.0045\text{--}0.5 \text{\AA}^{-1}$ for the measurements and analysis.³⁴ The q and the intensity were recorded using a two-dimensional detector placed at 90° to the incident neutron beam. Data from the samples were placed on an absolute scale by normalizing the scattered intensity to the incident beam flux. Finally, the data were radially averaged to produce scattered intensity, $I(q)$, versus q plots. In all of the cases, the instrument and buffer backgrounds were subtracted from the sample scattering. The structural parameters of Rec1-resilin were determined from SANS data fits using the “SasView” program (<http://www.sasview.org/>).

$I(q)$ is proportional to the product of the structure factor $S(q)$ and the form factor $P(q)$, which may be expressed as follows³⁵

$$I(q) = \left(\frac{C_2 M}{N_A} (\Delta\rho)^2 \gamma^2 \right) P(q) S(q) \quad (2)$$

where “ M ” is the molecular weight of the protein, “ C_2 ” is the concentration, “ γ ” is the molecular volume of the protein, and “ $\Delta\rho$ ” is the scattering contrast, the protein–solvent electron scattering length density (SLD) difference in the case of SAXS and the difference between the neutron SLD of the protein and that of the D_2O buffer (i.e., $\Delta\rho = \rho_{\text{pro}} - \rho_{\text{buf}}$) in the case of SANS. In the case of SANS, ρ_{buf} was taken for 10 mM PBS in D_2O ($6.3115 \times 10^{-6} \text{\AA}^{-2}$, calculated using online neutron activation and a scattering calculator; <https://www.ncnr.nist.gov/resources/activation/>), whereas ρ_{pro} was determined as $2.8 \times 10^{-6} \text{\AA}^{-2}$ (which corresponds to a typical SLD value for Rec1-resilin in 100% D_2O), using the Science and Technology Facilities Council online biomolecular SLD calculator (<http://pslcc.isis.rl.ac.uk/Pslcc/>). A mean density of 1.41 g cm^{-3} was used for the calculation of the volume fraction of Rec1-resilin in solution.³⁶ $P(q)$ is a q -dependent orientation-averaged function

that provides information about the size and shape of the protein. $S(q)$ provides information about the orientation-averaged protein–protein interactions.³⁵ The $I(q)$ of a concentrated protein solution is expected to be a function of both the protein’s $P(q)$, which is determined by its size and shape, and the intermolecular $S(q)$, which is sensitive to the intermolecular interaction potential. To extract $S(q)$ from the scattering signal, the scattering patterns of both diluted and highly concentrated protein solutions were recorded.

To obtain model-independent structural information of the protein, from both SAXS and SANS, the scattering intensities in a very low q region were extrapolated to zero concentration using the Guinier approximation (eq 3)²⁸

$$I(q) = I(0) \exp\left(-\frac{q^2 R_g^2}{3}\right); \quad (q_{\max} \cdot R_g \leq 1) \quad (3)$$

where $I(q)$ is the intensity of scattering, $I(0)$ is the intensity at zero q (which is proportional to both the mass concentration and the molecular mass of the particles), and R_g is the radius of gyration of the protein in solution. The fractal dimension and equilibrium structure qualities were evaluated from a relatively larger q region using the Porod relationship

$$I(q) \propto q^{-D_m} \quad (4)$$

where D_m is a constant that reflects the distribution of interatomic distances on different length scales and provides information about the internal scaling of interatomic distances, without reference to other proteins or specific models, and can be interpreted as a fractal dimension. For polymers, D_m is related to the Flory exponent, $\nu = 1/D_m$, which describes the relationship between polymer chain length and R_g according to

$$R_g = R_0 N^\nu \quad (5)$$

where N is the number of residues in the chain and R_0 is a constant, which is a function of, among other things, the persistence length of the polymer.^{37,38} The value of D_m , or equivalently ν , reflects the degree of compaction of the chain, is sensitive to the energetic balance between intramolecular interactions and interactions with the solvent, and gives an indication of the “unfoldedness” or “random coil” status of Rec1-resilin in the solution. The scattering data were qualitatively assessed by means of a Kratky ($\ln I(q) \times q^2$ vs q) plot.

The quantification of the structural parameters of the experimental protein samples from SAS relies on the regression of different models for protein–protein interactions and is limited to the availability of suitable models and simple protein geometries to capture the entire set of experimental conditions.³⁹ The SAS curves were fitted with different theoretical models to elucidate the structure, morphology, and organization of Rec1-resilin in three-dimensional (3D) space.

3. RESULTS AND DISCUSSION

3.1. Effect of Crowding on Conformational Ensembles of Rec1-Resilin. Figure 1A shows the double-logarithmic concentration-normalized SAXS intensity profile, $I(q)$ (I_q/C_p , where I_q is the scattering intensity and C_p is the protein concentration), of as-synthesized Rec1-resilin in dilute to dense solution states measured at physiological pH and at 25 °C. The use of normalized intensity profile removes the trivial concentration dependence, and the effect of protein crowding can be illustrated more rationally. It is clear from Figure 1A that the overall shape of the SAXS profile is remarkably insensitive to the increase in concentration. The figure illustrates that in the higher- q regime ($q > 0.09 \text{ \AA}^{-1}$), where intramolecular scattering dominates, the I_q/C_p value is independent of C_p . Moreover, the absence of any correlation peak and that of a sharp intensity increase in the lower- q ($q \lesssim 0.02 \text{ \AA}^{-1}$) region of the SAXS profile, even at a very high protein concentration level (>20 wt %), reveal the absence of any stable secondary structure and any large aggregation within the experimental SAXS window range. Noticeably, a progressive decrease in the lower q intensity, $q \lesssim 0.05 \text{ \AA}^{-1}$ (sensitive to protein–protein correlation and with increase in solution concentration), without appearance of any pronounced correlation peak within the experimental q range was observed. In an ideal solution in which the protein molecules are well separated from each other, there is no position or orientation correlation between them, that is, the $S(q) = 1$, and total scattering has contributions only from $P(q)$. With increasing protein concentration and crowding, the interference effect between proteins cannot be neglected and the $S(q)$ may become an important contributor in the total scattering intensity (eq 2). The $S(q)$ in the low- q range strongly depends on the interaction potential between protein molecules, and the $S(q)$ at the origin, $S(q) = 0$, is equal to the normalized osmotic compressibility.⁴⁰ The progressive decrease in the concentration-normalized $I(q)$ in the low- q regime, with increasing concentration, reflects the presence of a repulsive intermolecular interaction and uniform distribution of protein molecules. Dutta et al.⁶ have reported that the surface charge of Rec1-resilin at physiological pH is negative and therefore the presence of repulsive interaction is expected. However, the steric repulsion between impenetrable macro-

molecules in a crowded medium is a major factor in determining the final compact structure.

The average apparent R_g (root mean square average of the values for the individual molecule/particle of any shape) was estimated applying Guinier approximation in a very low q region (calculated from the slope of the linear region ($\ln(I)$) versus q^2 plot, Figure 1B). This relationship is valid for $q \leq 1/R_g$, depending somewhat on the shape of the particle. The R_g of 1 wt % Rec1-resilin solution determined using the model-independent Guinier approximation is $4.93 \pm 0.16 \text{ nm}$ (Figure 1B and Table 1), which is close to the previously reported value

Table 1. Structural Fit Parameters of SAXS Intensity Profile of Rec1-Resilin as a Function of Concentration at pH 7.4 and 25 °C

concentration (wt %)	Guinier R_g (nm)	Porod slope
1	4.93 ± 0.16	1.98 ± 0.01
5	4.92 ± 0.06	1.95 ± 0.01
10	4.99 ± 0.06	1.95 ± 0.02
15	4.35 ± 0.04	1.91 ± 0.02
20	3.49 ± 0.04	1.89 ± 0.02
25	3.04 ± 0.03	1.75 ± 0.02
30	2.91 ± 0.01	1.74 ± 0.02

of $\sim 5.09 \text{ nm}$ for freeze-dried Rec1-resilin in dilute solution.¹⁴ Rec1-resilin displayed constant R_g values from very dilute up to 10 wt % concentrations (Figure 1B and Table 1). Consequently, significant intermolecular interactions are not reflected, and the total scattering intensity may be considered as the sum of the scattering of the individual molecules.¹² However, with a further increase in concentration above this threshold value, the Guinier R_g value decreased progressively with increase in concentration, and for 30 wt % solution, the R_g value decreases to $2.91 \pm 0.01 \text{ nm}$ (Table 1).

The scattering profile from the intermediate q ($0.05 \text{ \AA}^{-1} \leq q \leq 0.15 \text{ \AA}^{-1}$) contains information about the distribution of the interatomic distances within a molecule. For many different particle types, a Porod plot, $\log I(q)$ versus $\log q$ (eq 4), within this q -range displays a linear relationship, and D_m can be directly estimated from the SAXS profile. The slope of the plot represents the distribution of interatomic distances on different length scales, and it can be interpreted in terms of D_m . This parameter of the scattering objects represents the scaling relationship between the mass enclosed by a volume and the linear dimensions of the volume and provides information about the local structure and quality of the surface, texture, and interface. D_m is sensitive to favorable or unfavorable solvation of the chain, with larger values reflecting unfavorable interactions with solvent. D_m for a well-solvated polymer chain is predicted to approach ~ 1.7 . The measured Porod slope (D_m) of 1 wt % solution of Rec1-resilin is observed to be 1.98 ± 0.01 (Table 1), which is the signature of a Gaussian chain in a dilute environment (without excluded-volume effects), for a random-flight chain in a Θ -solvent or in an ideal solvent ($D_m = 2$).²¹ It is striking that with a progressive increase in the solution concentration, the D_m value decreases steadily (Table 1), and for 30 wt % solution, it displays the characteristics of a fully swollen coil ($D_m = 1.74 \pm 0.02$), where the chain interacts equally well with itself and the solvent.³⁷ If compact conformations are favored, with increasing concentration and crowding, a progressive increase in the fractal dimension is expected. The Kratky plot shown in Figure 1C also supports

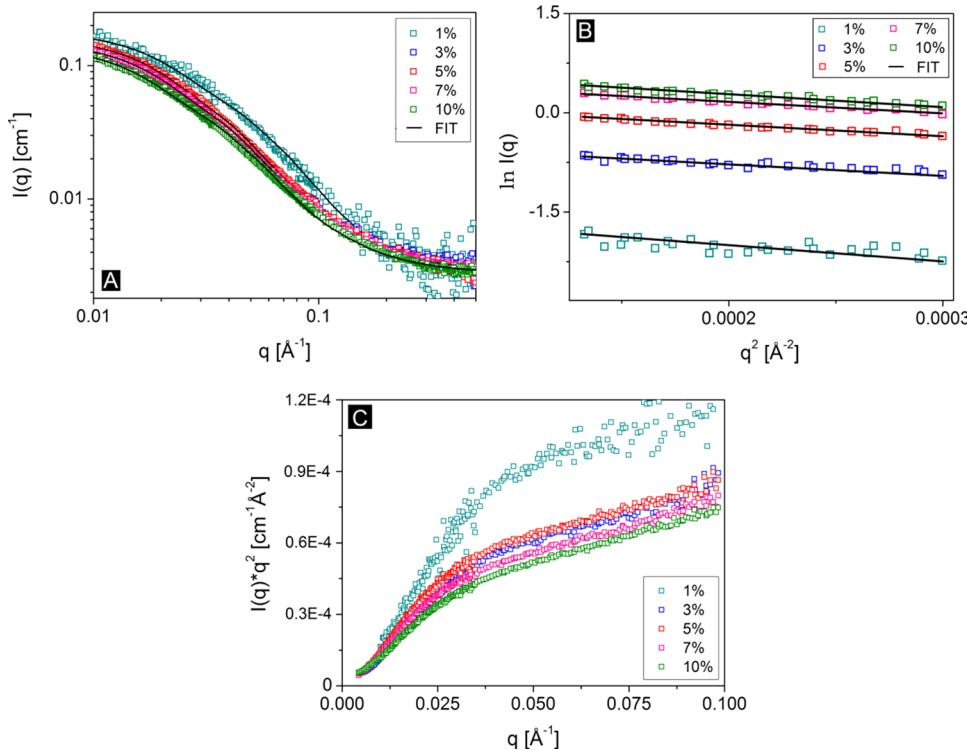


Figure 2. (A) Experimental SANS intensity profile normalized to 1 wt % Rec1-resilin solution (a scattering function for triaxial ellipsoid particles was used for curve fittings and the lines represent the best-fitted curves to $I(q)$ for the respective concentration), (B) corresponding Guinier approximation, and (C) Kratky plot of Rec1-resilin solutions as a function of concentration at pH 7.4 and 25 °C.

Table 2. Structural Fit Parameters of Rec1-Resilin SANS Intensity Profile as a Function of Concentration at pH 7.4 and 25 °C

conc. (%)	volume fraction of Rec1	shape-independent fit			triaxial ellipsoid fit					
		Guinier R_g (nm)	Gaussian R_g (nm)	Porod slope	semiaxis A (nm)	semiaxis B (nm)	semiaxis C (nm)	SLD ellipse (10^{-6} Å ⁻²)	V_E ^a	R_g (nm)
1	0.007	5.90 ± 2.00	6.50 ± 0.06	1.75 ± 0.04	0.4	3.35 ± 0.06	14.50 ± 0.30	4.62	0.46	6.70
3	0.021	6.10 ± 0.90	7.40 ± 0.03	1.70 ± 0.01	0.4	4.00 ± 0.03	15.10 ± 0.10	4.68	0.45	7.00
5	0.035	6.60 ± 0.60	8.20 ± 0.02	1.70 ± 0.01	0.4	4.40 ± 0.02	16.90 ± 0.10	4.73	0.43	7.80
7	0.050	7.40 ± 0.70	8.20 ± 0.01	1.70 ± 0.01	0.4	4.50 ± 0.02	18.30 ± 0.10	4.77	0.42	8.40
10	0.071	7.50 ± 0.60	8.20 ± 0.01	1.70 ± 0.01	0.4	4.20 ± 0.01	18.80 ± 0.10	4.89	0.39	8.60

^aVolume fraction of protein contributing to SLD ellipse.

the Gaussian chain structure quality for Rec1-resilin in solution with an initial monotonic increase in the low- q region followed by a plateau in the high- q region. With an increase in crowding, a progressive transformation in the structure qualities of Rec1-resilin from a Gaussian chain to a fully swollen coil was also observed, which is reflected from the respective decrease in the slope of the initial monotonic increase in low- q intensity, concomitant with the progressive increase in slope at higher q in the Kratky plot (Figure 1C).

The change in the distribution of interatomic distances and equilibrium molecular size of Rec1-resilin with concentration was also determined using the pair-distance distribution function, $P(r)$ (Figure 1D). $P(r)$ is a histogram of all of the interatomic distances (r) calculated by inverse Fourier transform of the SAXS intensity.²¹ $P(r)$ may be considered as more appropriate for R_g representation for IDPs than Guinier's approximation because $P(r)$ is a model-independent function that includes the entire experimental scattering spectrum. A similar approach has been adopted by other researchers to describe an unfolded chain,⁴¹ where Guinier's law is less appropriate and often underestimates the R_g values of extended

chains. The $P(r)$ of Rec1-resilin (Figure 1D) displays characteristics of extended conformations of the protein molecules in aqueous solution with maximum molecular dimension (D_{\max}) of ~23 nm for 1 wt % of Rec1-resilin.⁴² With an increase in concentration and crowding, a progressive decrease in D_{\max} along with progressive narrowing of the distribution and a peak shift toward low " r " supports the estimated decrease in R_g with increased concentration (Figure 1D). Overall, the SAXS data confirm that Rec1-resilin is an IDP in a dilute solution state and it retains overall IDP nature even at higher concentration with no major conformational change; however, a molecular compaction related to a repulsive intermolecular potential is evident.

Figure 2A shows the double-logarithmic SANS intensity profile of Rec1-resilin (from 1 to 10 wt %) as a function of concentration and reflects its evolution from semidilute to concentrated solutions at physiological pH and 25 °C. SANS was employed in exactly the same way as SAXS (without contrast matching) in D₂O. The difference is that SAXS examines electron-density fluctuations and in SANS neutrons identify hydrogen-density fluctuations. From Figure 2A, it is

clear that the overall SANS profile of the Rec1-resilin solutions remains similar between 1 and 10 wt %. These overall SANS (Figure 2A) and SAXS (Figure 1A) profiles are also similar in a wide q range, although there are some differences. The apparent R_g of Rec1-resilin determined as a function of concentration using both Guinier approximation (eq 3) and shape-independent Gaussian coil scattering function fits⁴³ and the Porod slope are given in Table 2. As has been identified for SAXS, SANS $I(q)$ in the low- q regime decreases with an increase in solution concentration because of the presence of repulsive interaction. The observed differences between the R_g values estimated from SAXS and SANS (R_g from SANS is relatively higher) are likely to be promoted by the inclusion of D₂O in the protein samples. It has been reported that although the chemical characteristics of D₂O is the same as those of H₂O, the H/D exchange increases the stability of the deuterated protein contributing to the prolonged stable state and may contribute to the change in the conformational ensemble. On the basis of quantum chemical calculation, it has been reported that isotopic substitution of H by D lowers the total energy of hydrophilic amino acids because of the decrease in zero-point vibration energy. When H is replaced with D in a biological molecule, the C–D bond is about 10 times stronger than the C–H bond.^{44,45} A Porod slope of 1.70 ± 0.01 , which is insensitive within the experimental concentration range, confirmed an equilibrium intrinsic structure quality of a fully swollen coil at neutral pH (Table 2).

To gain further insights into the conformational changes and organization of Rec1-resilin in detail in 3D space, the SANS profiles were fitted with different appropriate computational models including sphere, cylinder, ellipsoid, elliptical cylinder, and triaxial ellipsoid (Figure S2 illustrates some typical model fitting). The quantification of 3D structural parameters of proteins from SAS relies on regression of different models for protein–protein interactions and is limited to the availability of suitable models and simple protein geometries to capture the entire set of experimental conditions.³³ In the past few years, there has been an incredible increase in the success of SAS due to the latest advances in computational data analysis. Nevertheless, SAS is confronted with the ill-posed problem of inferring a 3D structure from a one-dimensional scattering profile. The universal strategy to infer a reliable model for an IDP is to impose constraints on the reconstructions by adding external information from complementary methods. This approach is extremely powerful and could provide highly important clues on the structural organization and ensemble. To compare the computational and experimental results, different computation model were employed, and each of the calculated average profiles was fit to the experimental SANS data. The R_g values obtained from dilute solutions of Rec1-resilin using a triaxial ellipsoidal model (compared to those obtained using other models examined) were observed to be the most appropriate (Figure S2) and to match with the R_g values obtained from both Guinier and shape-independent Gaussian coil scattering function fits (Table 2). Therefore, the scattering function for a triaxial ellipsoidal model was used for all of the SANS fits, as shown in Figure 2A. The R_g values were obtained from the triaxial ellipsoid structural fit parameters of axes A, B, and C (where A < B < C) using eq 6⁴⁶

$$R_g^2 = \frac{1}{5}[A^2 + B^2 + C^2] \quad (6)$$

Semiaxis A was fixed to 0.4 nm on the basis of the goodness of several fits tested for the measured concentrations (Figure S3) and the reported value of approximately 0.4 nm for the random coil.⁴⁷ From the axis values of the structural fit (Table 2), it can be concluded that Rec1-resilin takes the form of a typical triaxial ellipsoidal sheet in aqueous solution at physiological pH. Moreover, the SLD of the ellipsoid was observed to increase marginally with increase in concentration (Table 2), indicating a marginal increase in the hydration level of protein. Semiaxis C marginally increases with concentration, and the volume fraction of Rec1-resilin corresponding to the SLD of the ellipsoid is observed to decrease with protein concentration. The characteristics of the $I(q)$ at higher q and lower protein concentration depend only on the molecular dimensions and geometric structure of the protein, that is, on the $P(q)$. Therefore, at low concentrations, the SANS profile provides effectively only the $P(q)$ information because proteins are not very strong scatterers even in D₂O solutions. The Hansen and Hayter mean spherical approximation structure factor model (successful in studying the structures of charged colloidal dispersions in a dielectric medium)⁴⁸ was also used for the SANS fit of 10.0 wt % Rec1-resilin solution data to examine the extent of the influence of the structure factor, $S(q)$, on the data fit. The observation of no further improvement in curve fit and χ^2 value (Table S1) indicates the absence of significant $S(q)$ even for 10.0 wt % Rec1-resilin at physiological pH. It has been reported that for protein solutions qualitative features of protein–protein interactions in the $I(q)$ curves can be identified for low- and intermediate- q regions (i.e., $q \leq 0.1 \text{ \AA}^{-1}$) as long as both the strength of the interactions and protein concentration are not large enough for $S(q) \neq 1$.³⁵

At the molecular level, the solubility and the resulting conformational ensembles of proteins in aqueous buffers depend on the distribution of hydrophilic and hydrophobic amino acid residues on the protein surface. The major contribution involves a balance between the charge on a particular residue and the net surface charge and the water-binding ability of the amino acid residues. The composition of Rec1-resilin is mainly dominated by 18 copies of a 15-residue repeat sequence: GGRPSDSYGYAPGGGN. In the structure of Rec1-resilin, a Ser (position 5), a Tyr (position 8), a Gly (position 9), and a Pro (position 11) are conserved in all of the 18 copies (Figure S1A). It contains a very high content of Gly (~34.5 mol %) and Pro (~14%) and lacks hydrophobic residues with long aliphatic or aromatic side chains (Table S2). The amino acid residues in Rec1-resilin are dominated by hydrophilic residues including both uncharged, ~33% (Ser ~14.2%, Thr 1.6%, Asn 6.45%, Gln 3.87%, Tyr 6.45%), and charged polar, ~11.5% (with Asp ~4% and Arg ~5%), hydrophilic residues. As expected from the structural features of Rec1-resilin, a typical Kyte–Doolittle^{49,50} hydropathicity plot of the Rec1-resilin sequence demonstrates that all of the domains of Rec1-resilin exhibit values below zero, reflecting pronounced hydrophilicity of the protein surface (Figure S4). The unique combination of structural characteristics enables Rec1-resilin to be an IDP with outstanding flexibility, water solubility, and responsiveness as discussed in detail in our early report.⁶ Trevino et al.⁵¹ developed a set of experimentally derived general rules that highlight the contribution of individual amino acid residues in the protein structure to protein solubility and association. The contribution of the ionizable amino acid residues to protein solubility varies widely depending on the net charge of the protein, and at any specific

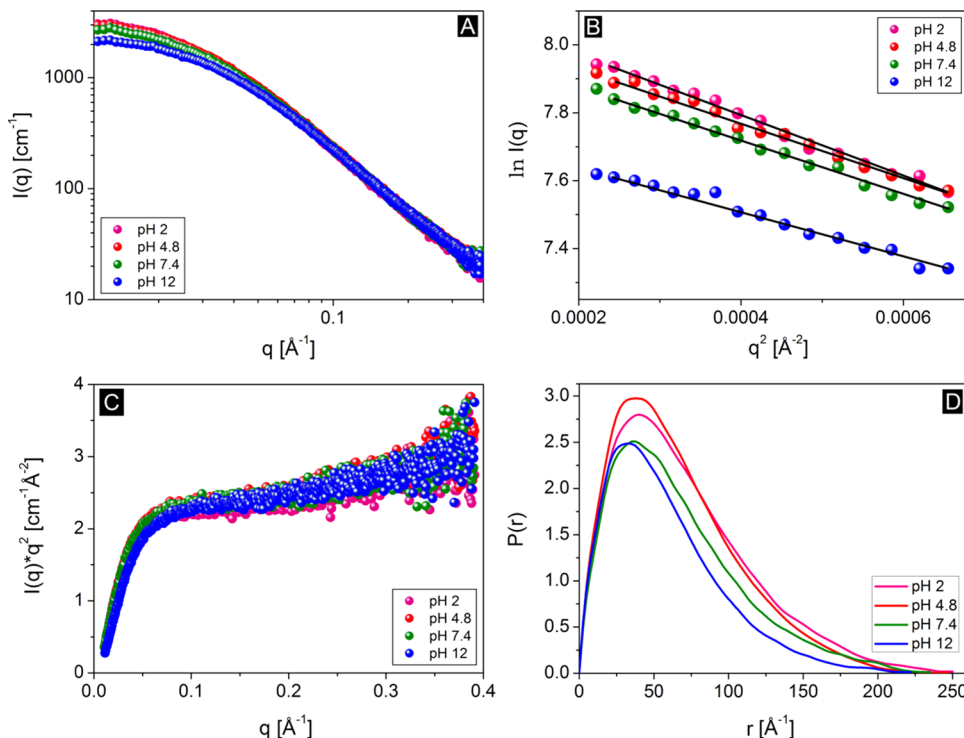


Figure 3. (A) SAXS intensity profile, (B) Guinier approximation, (C) Kratky plot, and (D) the pair-distance distribution function of 10 wt % Rec1-resilin as a function of pH at 25 °C.

pH, the net charge on a protein is determined by the pK values of the ionizable amino acids present. At physiological pH (pH relatively higher than 4.8; the experimental isoelectric point (IEP)),⁶ the ζ potential of Rec1-resin is -7.4 ± 1.7 mV,⁸ reflecting a marginal negative surface charge, and the charged amino acid residue Asp with a side chain $-\text{CH}_2\text{CO}_2\text{H}$ ($\text{p}K_a \sim 3.90$) contributes most favorably to its solubility. Among the nonionisable polar amino acid residues Ser, Asn, Gln, and Thr, only Ser affects the solubility favorably. The water molecules forming a solvation layer (bound water) around hydrophilic surface residues further enhance the solubility of Rec1-resilin at physiological pH. The experimental molecular condensation observed with protein crowding is mainly directed by the interplay among anisotropic confinement, steric repulsion, and osmotic pressure. The observed decrease in D_m and progressive increase in SLD with crowding reflect that high level of crowding promotes a more favorable interaction of the protein segment with water, which is related to the increased osmotic pressure with concentration at the cost of hydration enthalpy.

3.2. pH-Mediated Change in the Conformational Ensemble of Rec1-Resilin. Protein conformation and conformational ensembles may change dramatically with pH, and denaturation of protein may result in unfolding of protein, in which state the charged side groups are more exposed to the solvents and their effective pK values are closer to their intrinsic values.⁵² The experimental IEP of Rec1-resilin is observed to be at pH ~ 4.8 , and it demonstrates significant pH responsiveness including a dramatic change in surface charge, hydrodynamic characteristics, and photophysical properties such as ultraviolet absorption and fluorescence characteristics.⁶ This has been attributed to the change in protonation/deprotonation of the amino acid residues present. However, circular dichroism and SAXS spectra of very dilute solution of Rec1-resilin confirm no major change in the IDP nature of the protein molecules.¹⁴ To

elucidate the pH-responsive equilibrium structure, ensemble of conformations, and self-assembly of Rec1-resilin in a dense solution phase, the scattering curves of 10 wt % protein solution were elucidated at pH values of 2, 4.8, 7.4, and 12. Figure 3 shows the SAXS intensity profiles (Figure 3A), the Guinier approximation, (Figure 3B), the dimensionless Kratky plot (Figure 3C), and $P(r)$ (Figure 3D) of 10 wt % Rec1-resilin as a function of pH. The structural fit parameters of SAXS profiles are given in Table 3, and it can be observed that the

Table 3. Structural Fit Parameters of the SAXS Intensity Profile of Rec1-Resilin as a Function of pH and Temperature

conc. (%)	pH	temp. (°C)	Guinier R_g (nm)	Porod slope
10	2	25	5.21 ± 0.06	1.99 ± 0.01
10	4.8	25	5.07 ± 0.04	1.97 ± 0.07
10	7.4	25	4.99 ± 0.06	1.95 ± 0.02
10	12	25	3.88 ± 0.05	1.92 ± 0.01
5	7.4	4	6.24 ± 0.04	2.03 ± 0.01
5	7.4	25	4.92 ± 0.06	1.95 ± 0.01
5	7.4	75	3.57 ± 0.31	1.72 ± 0.03

Guinier R_g of Rec1-resilin, in a dense solution state, decreases with a change in pH from the IEP (pH = 4.8) toward the basic environment significantly, such as pH increased to 12. This decrease in R_g can be attributed to the increase in the reported negative surface charge of the protein and the increase in the repulsive interaction above the IEP, as reported by Dutta et al.⁶ and Truong et al.⁸ The negative surface charge of Rec1-resilin dramatically increases above pH 10 (ζ potential: -31.4 ± 6.5 mV at pH 10.7 relative to -7.4 ± 1.7 mV at pH 7.11) because of ionization of the side-chain hydroxyl of Tyr residues (~ 6.5 mol % of the Rec1-resilin sequence). The interprotein

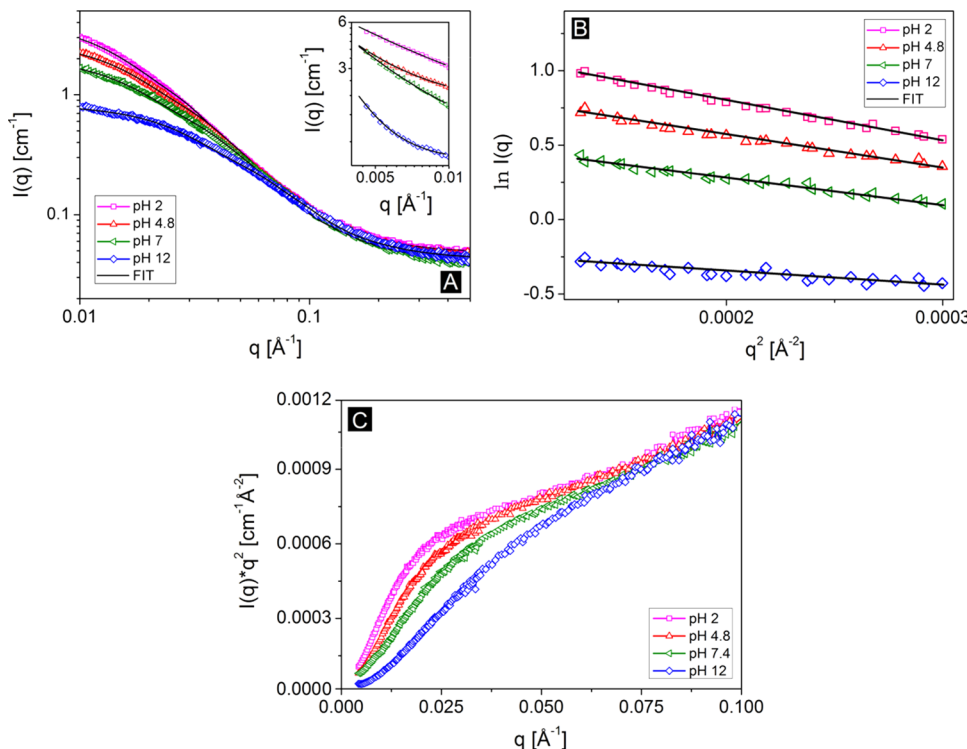


Figure 4. (A) SANS intensity profile; inset: the corresponding SANS intensity profile at an extended low- q region. A scattering function for triaxial ellipsoid particles was used for curve fittings. The solid lines represent the best-fitted curves to $I(q)$ for the respective pH. (B) Guinier approximation. (C) The Kratky plot of 10 wt % Rec1-resilin as a function of pH at 25 °C.

Table 4. Structural Fit Parameters of the SANS Intensity Profile of 10 wt % Rec1-Resilin as a Function of pH at 25 °C

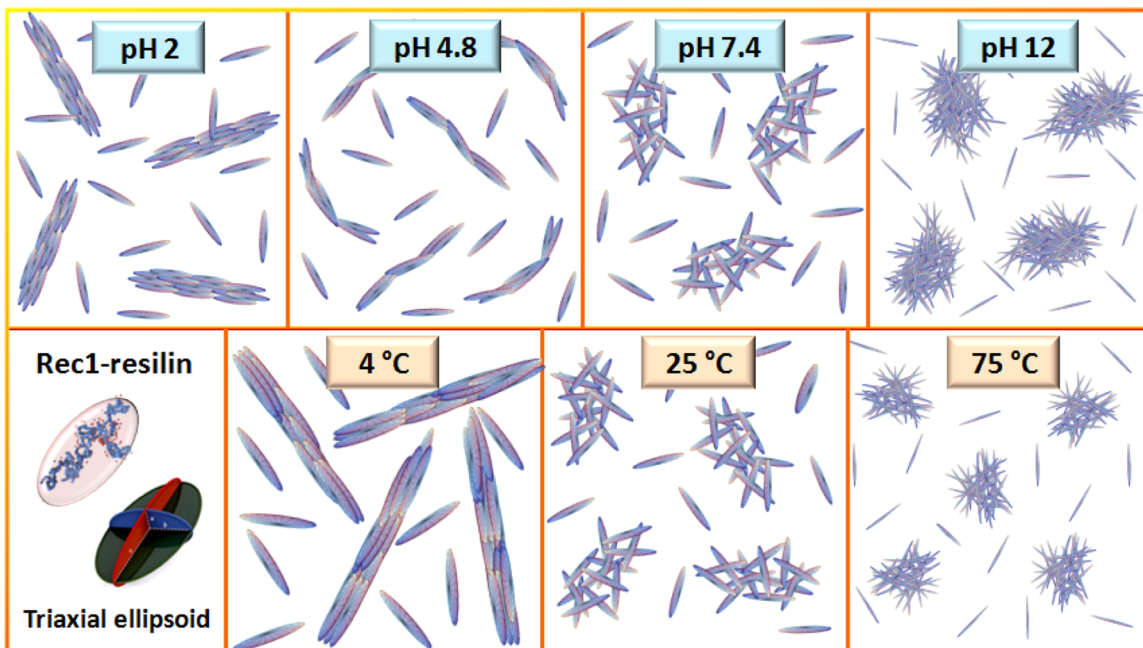
pH	shape independent fit			triaxial ellipsoid fit				
	Guinier R_g (nm)	Gaussian R_g (nm)	Porod slope	semiaxis A (nm)	semiaxis B (nm)	semiaxis C (nm)	SLD ellipse (10^{-6} Å^{-2})	R_g (nm)
2	10.60 ± 2.00	13.10 ± 0.03	1.82 ± 0.06	0.4	6.40 ± 0.01	26.70 ± 0.30	4.86	12.30
4.8	8.90 ± 1.10	10.20 ± 0.02	1.74 ± 0.02	0.4	5.10 ± 0.02	23.30 ± 0.24	4.87	10.60
7.4	7.50 ± 0.60	8.20 ± 0.01	1.70 ± 0.01	0.4	4.20 ± 0.01	18.80 ± 0.10	4.89	8.60
12	4.50 ± 0.40	5.10 ± 0.01	1.60 ± 0.07	0.4	2.70 ± 0.01	10.70 ± 0.05	4.87	4.90

repulsion was reflected from the decrease in SAXS intensity at low q with increase in pH (Figure 3A).

However, with change in pH, no significant change in the nature of the Kratky plot (initial monotonic increase in the low- q followed by a plateau in the high- q region in Figure 3C) and a marginal change in the Porod slope (1.95 ± 0.02 in Table 3) were observed. These observations support the fact that the protein structure is a stable Gaussian coil over a wide range of pH. The unimodal $P(r)$ with a long tail along with the decrease in D_{\max} value and the shift of the peak toward a lower r value with progressive increase in pH validate the estimated decrease in R_g with increase in pH (Figure 3D). However, the determined parameters are limited to the measured q region of the SAXS experiment ($0.012 \text{ Å}^{-1} < q < 0.39 \text{ Å}^{-1}$).

Figure 4 illustrates the SANS intensity profiles (Figure 4A), the Guinier approximation (Figure 4B), and the dimensionless Kratky plot (Figure 4C) of 10 wt % Rec1-resilin as a function of pH. There are some differences between the SANS cross sections and the SAXS profile (Figure 3) of the sample with change in pH, particularly the shape of the Rec1-resilin scattering curve differs in the low- and intermediate- q regime ($q < 0.06$) with pH. Rec1-resilin demonstrated an increased scattering intensity at low q at the IEP (pH 4.8), which corresponds to an increase in the resulting R_g and semiaxes B

and C (quantitative variables for the triaxial ellipsoidal model), compared to that at physiological pH (Table 4). This transformation is associated with a marginal increase in the fractal dimension of the scattering molecule with a Porod slope of 1.74 ± 0.02 , which is analogous to the reported relative structural compactness at IEP, where the solubility of protein decreases in water or salt solutions at the pH that corresponds to their IEP.⁸ With a further decrease in the pH to 2, Rec1-resilin demonstrated an increase in R_g with an increase in the corresponding semiaxes B and C . The intrinsic structural transformation at pH 2 was observed with a further increase in the Porod slope of 1.82 ± 0.06 , suggesting an equilibrium structure between a swollen coil and a Gaussian chain and a relatively compact structure compared to that at physiological pH (Porod slope of 1.70 ± 0.01) and at IEP (Porod slope of 1.74 ± 0.02). Rec1-resilin at acidic pH demonstrates a positive net surface charge with protonated Asp (~4 mol % with $pK_a = 3.9$) and Glu (~0.3 mol % with $pK_a = 4.07$) amino acid residues and a reduced hydrophilicity and hydration layer.⁶ It has been clearly demonstrated by Kramer et al.⁵³ that negative surface charge had the strongest correlation with increased protein solubility because of the strong water-binding properties of Asp and Glu. They also reported no correlation between solubility and positive surface charge. The trend was also consistent with

Scheme 1. Schematic Representation of the Global Structural Changes Induced by the Environment^a

^aTop panel: effect of change in pH; bottom panel: effect of temperature.

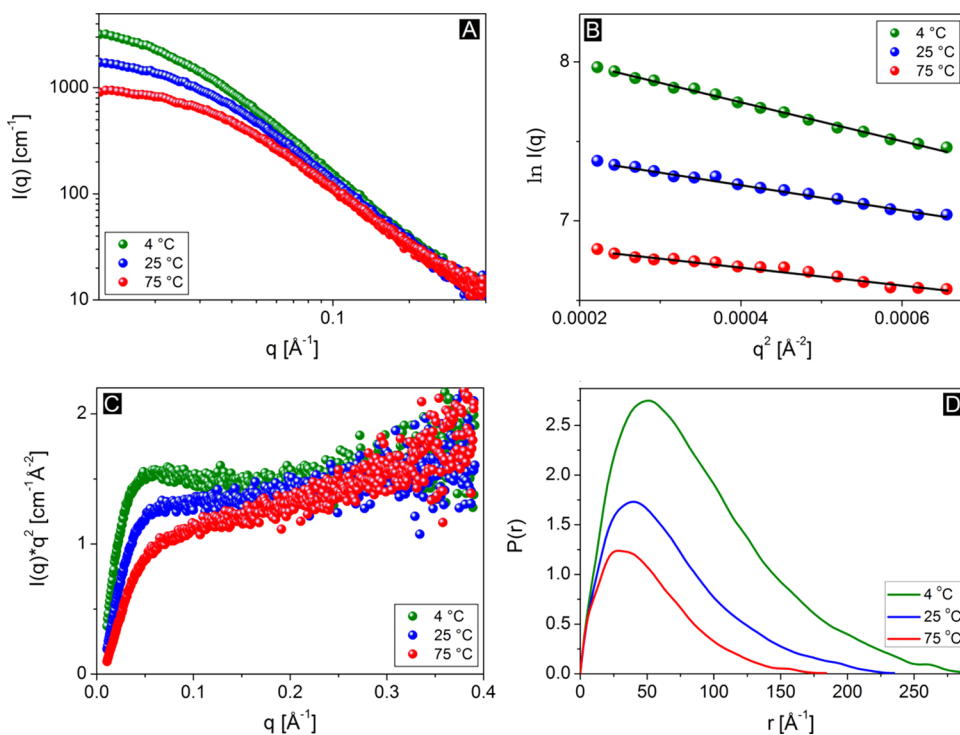


Figure 5. (A) SAXS intensity profiles, (B) Guinier approximation, (C) Kratky plot, and (D) pair-distance distribution function of 5 wt % Rec1-resilin as a function of temperature at pH 7.4.

the observed initial monotonic increase in the lower- q region of the Kratky plot with decrease in pH (Figure 4C).³⁸ On the contrary, an increase in the pH to 12 demonstrated a significant decrease in semiaxes B and C and the resulting R_g . At pH 12, the surface charge of Rec1-resilin is highly negative (the negative ζ potential value increases dramatically above pH 10.5) due to the deprotonation of all amino acid residues including tyrosine, Tyr (~ 6.5 mol % with $pK_a \sim 10.5$).⁶ The

intrinsic structural transformation was observed with a decrease in the Porod slope (1.60 ± 0.07) and a linear steady slope in the low- q region of the Kratky plot, suggesting self-assembly of Rec1-resilin to a compact rodlike structure. The increase in the intensity and slope of the SANS data at low q indicates the formation of large aggregate structures (Figure 4A). Therefore, SANS curves were measured at an extended low- q region ($0.0045\text{--}0.01 \text{\AA}^{-1}$), as shown in the inset of Figure 4A.

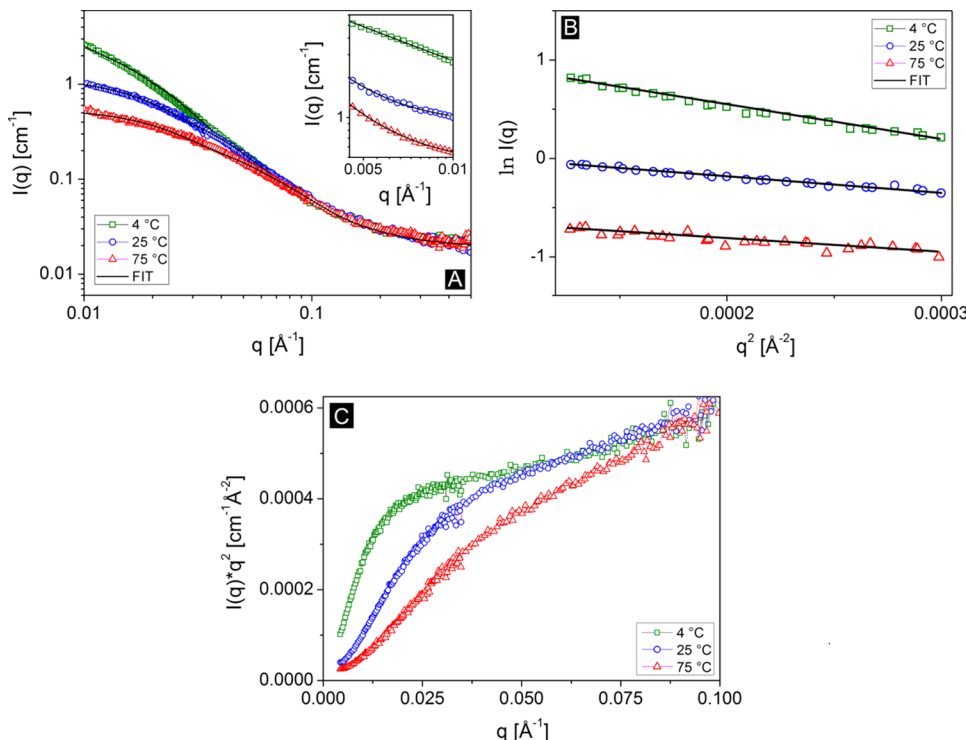


Figure 6. (A) SANS intensity profile; inset: the corresponding SANS intensity profile at an extended low- q region. A scattering function for triaxial ellipsoid particles was used for curve fittings. The solid lines represent the best-fitted curves to $I(q)$ for the respective temperature, (B) Guinier approximation, and (C) Kratky plot of 5 wt % Rec1-resilin as a function of temperature at pH 7.4.

A low- q slope of 2.60 ± 0.43 at physiological pH (determined using the absolute power law fit at an extended low- q region) demonstrated that Rec1-resilin triaxial ellipsoidal units organized into a large partially collapsed coil-like structure. At pH ~ 4.8 (IEP), the determined low- q -slope value of 1.80 ± 0.18 indicated the organization of Rec1-resilin triaxial ellipsoidal sheets to exhibit qualities of a large swollen coil structure. Moreover, a decreased low- q -slope value (1.10 ± 0.15) estimated at pH 2 demonstrated the structural organization of Rec1-resilin triaxial ellipsoidal units to form a large rigid-rodlike structure. On the contrary, at pH 12, Rec1-resilin triaxial ellipsoidal sheets organized into a large compact mass fractal structure with rough interfaces (low- q slope of 3.50 ± 0.28). Therefore, it is evident that in the dense phase Rec1-resilin self-assembles and organizes to form a larger structure, which is pH-dependent and reversible. A schematic representation of the global structural changes induced by pH is shown in Scheme 1 (top panel). The size range that could be measured is limited to the presented SANS data and could be further extended using ultra-SANS in a future study.⁵⁴

3.3. Conformational Transitions at the Lower Critical Solution Temperature (LCST) and the Upper Critical Solution Temperature (UCST) of Rec1-Resilin. Rec1-resilin is an unusually temperature responsive biomacromolecule. We have demonstrated, experimentally, that it displays a unique dual-phase-transition behavior (exhibits both UCST at ~ 6 °C and LCST at ~ 70 °C for 1 wt % solution). Moreover, the conformation ensemble of Rec1-resilin is observed to be highly stable over the range of temperature between UCST and LCST (from ~ 6 to 70 °C) with hydrodynamic diameter of ~ 10 nm.⁶ To better understand the temperature-responsive equilibrium structural conformation, the morphology and organization of Rec1-resilin, the scattering curves of 5 wt % Rec1-resilin were

measured below UCST (4 °C), at room temperature (25 °C), and above LCST (75 °C) using SAS. Figure 5 represents the SAXS intensity profiles (Figure 5A), the Guinier approximation (Figure 5B), the dimensionless Kratky plot (Figure 5C), and $P(r)$ (Figure 5D) of 5 wt % Rec1-resilin as a function of temperature. The structural fit parameters of SAXS profiles are given in Table 3. Below the UCST, Rec1-resilin exhibits a sharp increase in scattering intensity, relative to that at room temperature (Figure 5A), supporting the reported UCST of Rec1-resilin in aqueous solution.⁶ From Table 3, it can be observed that the R_g of Rec1-resilin (Figure 5B) is higher below the UCST (4 °C), whereas it is lower above the LCST (75 °C), relative to that at room temperature. This observation was in disagreement with the measured hydrodynamic diameter above the LCST, observed using the dynamic light scattering (DLS) technique.⁶ Moreover, the measured Porod slope was observed to decrease with increase in temperature, suggesting intrinsic structural transformation of protein from a Gaussian coil (4 and 25 °C) to a fully swollen coil at 75 °C. The Kratky plot (Figure 5C) supports this structural transformation, showing a sharp increase in $I(q) \times q^2$ in the low- q region with decrease in temperature. In the mid- q region, a monotonic increase in Kratky plots indicates an IDP nature. Interestingly, the Kratky plot for Rec1-resilin at 4 °C presented a clear bump at $q = 0.05$ \AA⁻¹ followed by a flat region, the features that indicate a certain degree of compactness, and finally a continuous rise produced by the presence of disordered regions. A decrease in D_{\max} value and a shift of peak toward lower r in $P(r)$ validate the estimated decrease in R_g with increase in temperature (Figure 5D). However, the determined parameters are from the limited q region of SAXS (0.012 \AA⁻¹ $< q < 0.39$ \AA⁻¹).

To elucidate the equilibrium structure, morphology, self-assembly, and organization of Rec1-resilin at the UCST and

Table 5. Structural Fit Parameters of the SANS Intensity Profile of 5 wt % Rec1-Resilin as a Function of Temperature at pH 7.4

temp. (°C)	shape independent fit			triaxial ellipsoid fit				R_g (nm)
	Guinier R_g (nm)	Gaussian R_g (nm)	Porod slope	semiaxis A (nm)	semiaxis B (nm)	semiaxis C (nm)	SLD ellipse (10^{-6} Å^{-2})	
4	17.40 ± 4.00	18.90 ± 0.09	1.80 ± 0.01	0.4	8.80 ± 0.02	51.40 ± 0.90	4.70	23.3
25	6.60 ± 0.60	8.20 ± 0.02	1.70 ± 0.01	0.4	4.40 ± 0.02	16.90 ± 0.10	4.73	7.80
75	5.10 ± 0.50	5.60 ± 0.02	1.28 ± 0.05	0.4	2.80 ± 0.02	12.40 ± 0.90	4.78	5.70

LCST in dense solution phase, the scattering curves of 5 wt % Rec1-resilin solution were measured at 4, 25, and 75 °C using SANS. Figure 6A compares the SANS intensity data of 5 wt % Rec1-resilin solution at 4, 25, and 75 °C. It can be observed that the shape of the Rec1-resilin scattering curve at the low- q regime significantly differs ($q < 0.09 \text{ Å}^{-1}$) at each of these temperatures, implying a significant change. From Table 5, it can be observed that the R_g of Rec1-resilin at 4 °C increases almost 3-fold from 6.6 nm determined at 25 °C. This is in agreement with the significant increase in the hydrodynamic size of Rec1-resilin below the UCST forming aggregates, measured by DLS.⁶ The intrinsic structural transformation at 4 °C (below UCST) was observed with increase in the Porod slope (1.80 ± 0.01), suggesting an equilibrium structure between a swollen coil and a Gaussian chain (a relatively compact structure compared to that at room temperature, 25 °C, with Porod slope of 1.70 ± 0.01). Furthermore, from the structural fit parameters for the triaxial ellipsoid fit (Figure 6A and Table 5), it is determined that below UCST at 4 °C semiaxis B of Rec1-resilin increases by 2 times whereas semiaxis C almost increases by 3 times. However, the SLD at 4 °C was determined to be marginally lower than that at 25 °C. The increase in scattering and slope at low q indicates larger structure formation of Rec1-resilin at UCST. This observation clearly indicates that below UCST Rec1-resilin self-assemble to larger structural organization without much change in the overall molecular hydration level.

On the other hand, above LCST (75 °C), the scattering intensity was observed to be lower compared to that at 4 and 25 °C. Above LCST, the surface potential of Rec1-resilin may change as observed in An16-resilin,⁵⁵ another RMP, which possibly causes repulsion and decrease in intensity at low q with formation of protein-rich and protein-deficient regions (phase separation). The determined structural fit parameters (Table 5) indicated a decrease in both semiaxes B and C and the resulting R_g . The intrinsic structural transformation was observed with a significant decrease in Porod slope (1.28 ± 0.05) and a linear steady slope in the low- q region of Kratky plot (Figure 6B),⁵⁶ suggesting self-assembly of Rec1-resilin to form a structure close to that of a rigid rod. However, an increase in the hydrodynamic size of Rec1-resilin was observed and reported using DLS above the LCST.⁶ Therefore, SANS curves were measured in the extended low- q region ($0.0045\text{--}0.01 \text{ Å}^{-1}$), as shown in the inset of Figure 6A.

The power law fit at low q demonstrated a larger but a relatively compact structural organization of Rec1-resilin triaxial ellipsoidal sheets at 75 °C (above LCST) with a slope value of 2.67 ± 0.28 , which is greater than that of 2.59 ± 0.25 at 25 °C. The measured slope of 1.10 ± 0.01 at 4 °C (below UCST) demonstrated a rigid-rodlike structure of Rec1-resilin at 4 °C. Therefore, it is evident that Rec1-resilin self-assembles to form larger structures at both UCST and LCST relative to those at room temperature, which cannot be measured at a further low- q range and are limited to the presented SANS results. A

schematic representation of the global structural changes induced by temperature is shown in Scheme 1 (bottom panel).

Stimulus-triggered change in water solubility facilitates many directed self-assembling processes in nature including those in elastin and collagen fibers that impart important functional characteristics to extracellular matrix. Responsive synthetic polymers that exhibit phase behavior in water have also emerged as an important class of materials. The responsive properties of elastin-mimetic proteins that exhibit tunable LCST have stimulated the development of novel protein-based functional biomaterials for diverse applications.⁵⁷ Gelatin that displays UCST behavior has also been of significant importance in the food and pharmaceutical industries.⁵⁸ Dual-phase behavior (the occurrence of both UCST and LCST) in a single molecule was predicted by Li et al.⁵⁹ using a molecular model; however, it has not been reported experimentally. We have identified and reported Rec1-resilin as the first protein-polymer structure that exhibits intriguing dual-phase-transition behavior. Recently, Quiroz and Chilkoti⁵⁷ have provided heuristics for the prediction and encoding of phase behavior at the protein sequence level and attempted to synthesize several designer peptides that display both LCST and UCST transitions. From their work, they have postulated that Rec1-resilin's consensus repeat unit GRPSDSYGYAPGGGN is indeed a highly balanced fusion of a UCST motif GRPSDSYG (G-Xn-G) and a LCST motif APGGGN. Dutta et al.⁶ hypothesized that in Rec1-resilin the temperature-triggered self-assembly at UCST is related to the depletion of solvation layer (bound water) around the hydrophilic surface residues, specifically Asp (D), and the salting-out effect of the guanidino group bearing Arg (R). The observation of only a marginal change in SLD from SANS with temperature (Table 5) at 4 °C relative to that at room temperature indicates that the overall bound-water content does not change significantly at UCST. Quiroz and Chilkoti⁵⁷ have verified with ample evidence, using peptides with a designer sequence, that UCST in Rec1-resilin is related to a delicate balance of zwitterionic nature of the protein polymer and the intriguingly poor hydration of guanidinium ions in Arg, which is the major contributor to the hydrophobicity. They argued that the oppositely charged zwitterionic pair (Arg/Asp) in G-Xn-G motifs in the repeating sequence of Rec1-resilin facilitates bulk aggregation by minimizing the net charge of the polymer. Nevertheless, the large net charge on the protein polymer surface may experience substantial repulsive electrostatic interactions, and for self-assembly to occur, it must be out-competed by hydrophobic interactions, and the presence of Arg (accounts for a large fraction of the positively charged residues ~5 mol %) satisfies the requirement. A marked decrease in the UCST on disruption of the zwitterionic character of the UCST motif of Rec1-resilin by replacing Arg with Lys has also been identified.⁵⁷ Furthermore, the presence of a significant fraction of aromatic amino acids, Tyr (Y), both influences the hydrophobicity and introduces cation-π interactions between the Arg and Tyr residues.^{57,60} The observed progressive shift of UCST toward lower temperature

and complete lack of UCST phase transition of Rec1-resilin at >pH 10.5 (Figure S5) confirm the importance of the cationically charged Arg (pK_a of side chain ~12.5) for aggregation at UCST.

The aggregation of Rec1-resilin at higher temperature may be attributed to the nonspecific aggregation of the conformationally changed protein molecules. Rec1-resilin possesses a unique ensemble of structures, and at ~73 °C, the hydrophobic peptide residues of the Rec1-resilin molecule, which were buried within the interior of the structure, must become exposed to water. This thermodynamically unfavorable state is replaced by intermolecular association of the hydrophobic residues, resulting in a subsequent dramatic change in the hydrodynamic size through aggregation. Similar conformation changes of other proteins in aqueous solution induced by temperature have been observed by many investigators.^{55,61} Recently, we have also demonstrated that the LCST of Rec1-resilin can be controlled through the addition of hydrophobic polypeptides and native peptides.⁶²

4. CONCLUSIONS

The experimental data and the computational modeling work presented here confirm that Rec1-resilin displays the characteristics of an IDP with the features of a nonfolded overall random coil secondary structural conformation in aqueous solution. A monotonic increase in Kratky plots, relatively large R_g values, and expanded $P(r)$ functions with very large D_{\max} values were the key SAS features used to identify the IDP characteristics of the protein. It has been demonstrated that the conformational ensembles of Rec1-resilin do not change significantly with increase in concentration even up to 30 wt %. However, with increase in protein concentration above 10 wt %, the repulsive protein–protein intermolecular interaction dominates in a random environment, results in molecular compaction, and the R_g value decreases progressively with increase in concentration. The equilibrium structural features of Rec1-resilin were observed to be a swollen coil in concentrated solutions under physiological conditions and demonstrate its ability to form a rod to globular structural organization in aqueous solution as a function of pH and temperature (Scheme 1) that arises from its unique molecular composition, high degree of conformational dynamics, and its ability to interact with the environment with a high level of specificity. The scattering function for the triaxial ellipsoidal model was observed to best fit the experimental scattering data to provide a quantitative 3D description of the evolution of the conformational ensembles of Rec1-resilin with change in the environment and crowding.

■ ASSOCIATED CONTENT

Supporting Information

The Supporting Information is available free of charge on the ACS Publications website at DOI: [10.1021/acs.jpcb.6b02475](https://doi.org/10.1021/acs.jpcb.6b02475).

Structural consensus and alignment of amino acid repeat sequence in Rec1-resilin and MALDI-TOF mass spectra; various computational model fits for the experimental SANS intensity profile; triaxial ellipsoidal fits with various parameters for the measured experimental SANS intensity profile; Kyte–Doolittle hydropathicity plot of the Rec1-resilin sequence; effect of pH on the UCST (Figure S1–Figure S5); structural fit parameters of the SANS intensity profile of Rec1-resilin as a function of

structure factor (Table S1); amino acid composition of rec1-resilin (Table S2)

■ AUTHOR INFORMATION

Corresponding Author

*E-mail: naba.dutta@adelaide.edu.au, naba.dutta@unisa.edu.au.
Phone: +61 8 83134116, +61 8 83023546. Mobile: +61 0450042147.

Author Contributions

R.B. and N.K.D. designed the experiments. R.B., R.K., and J.M. performed the experiments. C.M.E. synthesized Rec1-resilin and edited the paper. R.B., N.K.D., R.K. (in part), J.M. (in Part), and N.R.C. (in part) analyzed the data. R.B. wrote the draft with N.K.D. and N.R.C., and the manuscript was finalized through contributions of all authors. All authors have given approval to the final version of the manuscript.

Notes

The authors declare no competing financial interest.

■ ACKNOWLEDGMENTS

This work was financially supported by the Australian Research Council (ARC) Discovery grants DP1092678 and DP120103537. Access to SANS (Quokka) and SAXS facility at the ANSTO was supported through an ANSTO beam time award (proposal 3606).

■ REFERENCES

- (1) Elvin, C. M.; Carr, A. G.; Huson, M. G.; Maxwell, J. M.; Pearson, R. D.; Vuocolo, T.; Liyou, N. E.; Wong, D. C. C.; Merritt, D. J.; Dixon, N. E. Synthesis and Properties of Crosslinked Recombinant Pro-Resilin. *Nature* **2005**, 437, 999–1002.
- (2) Ardell, D. H.; Andersen, S. O. Tentative Identification of a Resilin Gene in *Drosophila Melanogaster*. *Insect Biochem. Mol. Biol.* **2001**, 31, 965–970.
- (3) Whittaker, J.; Balu, R.; Choudhury, N. R.; Dutta, N. K. Biomimetic Protein-Based Elastomeric Hydrogels for Biomedical Applications. *Polym. Int.* **2014**, 63, 1545–1557.
- (4) Balu, R.; Whittaker, J.; Dutta, N. K.; Elvin, C. M.; Choudhury, N. R. Multi-Responsive Biomaterials and Nanobioconjugates from Resilin-Like Protein Polymers. *J. Mater. Chem. B* **2014**, 2, 5936–5947.
- (5) Li, L.; Kiick, K. L. Resilin-Based Materials for Biomedical Applications. *ACS Macro Lett.* **2013**, 2, 635–640.
- (6) Dutta, N. K.; Truong, M. Y.; Mayavan, S.; Roy Choudhury, N.; Elvin, C. M.; Kim, M.; Knott, R.; Nairn, K. M.; Hill, A. J. Genetically Engineered Protein Displays Multistimuli Responsive Behaviour. *Angew. Chem., Int. Ed.* **2011**, 50, 4428–4431.
- (7) Dutta, N. K.; Choudhury, N. R.; Truong, M. Y.; Kim, M.; Elvin, C. M.; Hill, A. J. Physical Approaches for Fabrication of Organized Nanostructure of Novel Resilin-Mimetic Elastic Protein Rec1-Resilin. *Biomaterials* **2009**, 30, 4868–4876.
- (8) Truong, M. Y.; Dutta, N. K.; Choudhury, N. R.; Kim, M.; Elvin, C. M.; Hill, A. J.; Thierry, B.; Vasilev, K. A. pH-Responsive Interface Derived from Resilin-Mimetic Protein Rec1-Resilin. *Biomaterials* **2010**, 31, 4434–4446.
- (9) Dutta, N. K.; Choudhury, N. R.; Mayavan, S.; Balu, R.; Whittaker, J.; Elvin, C. M.; Hill, A. J. Template Directed Formation of Metal Nanoparticles and Uses Thereof. WO Patent 2014071463A1, May 15, 2014.
- (10) Dutta, N. K.; Choudhury, N. R.; Balu, R.; Elvin, C. M.; Hill, A. J. Formation of Sub-Nano Metal Particles. WO Patent 2015024063A1, February 26, 2015.
- (11) Balu, R.; Bourgeois, L.; Elvin, C. M.; Hill, A. J.; Choudhury, N. R.; Dutta, N. K. A Multi-Responsive Intrinsically Disordered Protein (IDP)-Directed Green Synthesis of Fluorescent Gold Nanoclusters. *J. Mater. Chem. B* **2015**, 3, 6580–6586.

- (12) Mayavan, S.; Dutta, N. K.; Roy Choudhury, N.; Kim, M.; Elvin, C. M.; Hill, A. J. Self-Organization, Interfacial Interaction and Photophysical Properties of Gold Nanoparticle Complexes Derived from Resilin-Mimetic Fluorescent Protein Rec1-Resilin. *Biomaterials* **2011**, *32*, 2786–2796.
- (13) Truong, M. Y.; Dutta, N. K.; Choudhury, N. R.; Kim, M.; Elvin, C. M.; Nairn, K. M.; Hill, A. J. The Effect of Hydration on Molecular Chain Mobility and the Viscoelastic Behavior of Resilin-Mimetic Protein-Based Hydrogels. *Biomaterials* **2011**, *32*, 8462–8473.
- (14) Balu, R.; Knott, R.; Cowieson, N. P.; Elvin, C. M.; Hill, A. J.; Choudhury, N. R.; Dutta, N. K. Structural Ensembles Reveal Intrinsic Disorder for the Multi-Stimuli Responsive Bio-Mimetic Protein Rec1-Resilin. *Sci. Rep.* **2015**, *5*, 10896.
- (15) Dunker, A. K.; Obradovic, Z. The Protein Trinity: Linking Function and Disorder. *Nat. Biotechnol.* **2001**, *19*, 805–806.
- (16) Tompa, P. Intrinsically Unstructured Proteins. *Trends Biochem. Sci.* **2002**, *27*, 527–533.
- (17) Kurzbach, D.; Platzer, G.; Schwarz, T. C.; Hennen, M. A.; Konrat, R.; Hinderberger, D. Cooperative Unfolding of Compact Conformations of the Intrinsically Disordered Protein Osteopontin. *Biochemistry* **2013**, *52*, 5167–5175.
- (18) Uversky, V. N. Intrinsically Disordered Proteins from A to Z. *Int. J. Biochem. Cell Biol.* **2011**, *43*, 1090–1103.
- (19) Kato, M.; Han, T. W.; Xie, S.; Shi, K.; Du, X.; Wu, L. C.; Mirzaei, H.; Goldsmith, E. J.; Longgood, J.; Pei, J.; et al. Cell-free Formation of RNA Granules: Low Complexity Sequence Domains form Dynamic Fibers within Hydrogels. *Cell* **2012**, *149*, 753–767.
- (20) Van de Vondel, E.; Mensch, C.; Johannessen, C. Direct Measurements of the Crowding Effect in Proteins by Means of Raman Optical Activity. *J. Phys. Chem. B* **2016**, *120*, 886–890.
- (21) Svergun, D. I.; Koch, M. H. J.; Timmins, P. A.; May, R. P. *Small Angle X-Ray and Neutron Scattering from Solutions of Biological Macromolecules*; Oxford University Press: Oxford, U.K., 2013.
- (22) Johansen, D.; Jeffries, C. M. J.; Hammouda, B.; Trehewella, J.; Goldenberg, D. P. Effects of Macromolecular Crowding on an Intrinsically Disordered Protein Characterized by Small-Angle Neutron Scattering with Contrast Matching. *Biophys. J.* **2011**, *100*, 1120–1128.
- (23) Stradner, A.; Sedgwick, H.; Cardinaux, F.; Poon, W. C. K.; Egelhaaf, S. U.; Schurtenberger, P. Equilibrium Cluster Formation in Concentrated Protein Solutions and Colloids. *Nature* **2004**, *432*, 492–495.
- (24) Sinibaldi, R.; Ortore, M. G.; Spinozzi, F.; Carsughi, F.; Frielinghaus, H.; Cinelli, S.; Onori, G.; Mariani, P. Preferential Hydration of Lysozyme in Water/Glycerol Mixtures: A SANS Study. *J. Chem. Phys.* **2007**, *126*, 235101.
- (25) Stradner, A.; Cardinaux, F.; Schurtenberger, P. A Small-Angle Scattering Study on Equilibrium Clusters in Lysozyme Solutions. *J. Phys. Chem. B* **2006**, *110*, 21222–21231.
- (26) Svergun, D. I.; Richard, S.; Koch, M. H. J.; Sayers, Z.; Kuprin, S.; Zaccai, G. Protein Hydration in Solution: Experimental Observation by X-ray and Neutron Scattering. *Proc. Natl. Acad. Sci. U.S.A.* **1998**, *95*, 2267–2272.
- (27) Liu, Y.; Porcar, L.; Chen, J.; Chen, W. R.; Falus, P.; Faraone, A.; Fratini, E.; Hong, K.; Baglioni, F. J. Lysozyme Protein Solution with an Intermediate Range Order Structure. *J. Phys. Chem. B* **2011**, *115*, 7238–7247.
- (28) Lipfert, J.; Doniach, S. Small-Angle X-Ray Scattering from RNA, Proteins, and Protein Complexes. *Annu. Rev. Biophys. Biomol. Struct.* **2007**, *36*, 307–327.
- (29) Fitter, J.; Gutberlet, T.; Katsaras, J. *Neutron Scattering in Biology: Techniques and Applications*; Springer: Berlin, 2006.
- (30) Jacrot, B. The Study of Biological Structures by Neutron Scattering from Solution. *Rep. Prog. Phys.* **1976**, *39*, 911–953.
- (31) Zhang, F.; Runge, R. F.; Skoda, M. W. A.; Jacobs, R. M. J.; Wolf, M.; Callow, P.; Frielinghaus, H.; Pipich, V.; Prevost, S.; Schreiber, F. Hydration and Interactions in Protein Solutions Containing Concentrated Electrolytes Studied by Small-Angle Scattering. *Phys. Chem. Chem. Phys.* **2012**, *14*, 2483–2493.
- (32) Lyons, R. E.; Lesieur, E.; Kim, M.; Wong, D. C. C.; Huson, M. G.; Nairn, K. M.; Brownlee, A. G.; Pearson, R. D.; Elvin, C. M. Design and Facile Production of Recombinant Resilin-Like Polypeptides: Gene Construction and a Rapid Protein Purification Method. *Protein Eng., Des. Sel.* **2007**, *20*, 25–32.
- (33) Konarev, P. V.; Volkov, V. V.; Sokolova, A. V.; Koch, M. H. J.; Svergun, D. I. PRIMUS: A Windows PC-Based System for Small-Angle Scattering Data Analysis. *J. Appl. Crystallogr.* **2003**, *36*, 1277–1282.
- (34) Gilbert, E. P.; Schulz, J. C.; Noakes, T. J. ‘Quokka’—the Small-Angle Neutron Scattering Instrument at OPAL. *Phys. B: Condens. Matter* **2006**, *385*–*386*, 1180–1182.
- (35) Efimova, Y. M.; Well, A. A.; Hanefeld, U.; Wiercinski, B.; Bouwman, W. G. On the Neutron Scattering Length Density of Proteins in H₂O/D₂O. *Phys. B: Condens. Matter* **2004**, *350*, E877–E880.
- (36) Fischer, H.; Polikarpov, I.; Craievich, A. F. Average Protein Density is a Molecular-Weight-Dependent Function. *Protein Sci.* **2004**, *13*, 2825–2828.
- (37) Kohn, J. E.; Millett, I. S.; Jacob, J.; et al. Random-Coil Behavior and the Dimensions of Chemically Unfolded Proteins. *Proc. Natl. Acad. Sci. U.S.A.* **2004**, *101*, 12491–12496.
- (38) Glatter, O.; Kratky, O. *Small-Angle X-Ray Scattering*; Academic Press: London, U.K., 1982.
- (39) Rojas-Ochoa, L. F.; Castaneda-Priego, C. R.; Lobaskin, V.; Stradner, A.; Scheffold, F.; Schurtenberger, P. Density Dependent Interactions and Structure of Charged Colloidal Dispersions in the Weak Screening Regime. *Phys. Rev. Lett.* **2008**, *100*, No. 178304.
- (40) Tardieu, A.; Le Verge, A.; Malfois, M.; Bonneté, F.; Finet, S.; Kautz, R. M.; Belloni, L. Proteins in Solution: From X-ray Scattering Intensities to Interaction Potentials. *J. Cryst. Growth* **1999**, *196*, 193–203.
- (41) Bernado, P. Effect of Interdomain Dynamics on the Structure Determination of Modular Proteins by Small-Angle Scattering. *Eur. Biophys. J.* **2010**, *39*, 769–780.
- (42) Putnam, C. D.; Hammel, M.; Hura, G. L.; Tainer, J. A. X-ray Solution Scattering (SAXS) Combined with Crystallography and Computation: Defining Accurate Macromolecular Structures, Conformations and Assemblies in Solution. *Q. Rev. Biophys.* **2007**, *40*, 191–285.
- (43) Higgins, J. S.; Benoit, H. *Polymers and Neutron Scattering*; Clarendon Press: Gloucestershire, U.K., 1997.
- (44) Efimova, Y. M.; Haemers, S.; Wiercinski, B.; et al. Stability of Globular Proteins in H₂O and D₂O. *Biopolymer* **2007**, *85*, 264–273.
- (45) Sugiyama, T.; Yoshioka, T. Functional Difference between Deuterated and Protonated Macromolecules, Biochemistry, Genetics and Molecular Biology. In *Protein Structure*; Faraggi, E., Ed.; InTech Open: Rijeka, Croatia, 2012.
- (46) Feigin, L. A.; Svergun, D. I. *Structure Analysis by Small-Angle X-Ray and Neutron Scattering*; Springer: New York, 1987.
- (47) Qin, Z.; Buehler, M. J. Molecular Dynamics Simulation of the α -Helix to β -Sheet Transition in Coiled Protein Filaments: Evidence for a Critical Filament Length Scale. *Phys. Rev. Lett.* **2010**, *104*, 198304.
- (48) Hansen, J. P.; Hayter, J. B. A Rescaled MSA Structure Factor for Dilute Charged Colloidal Dispersions. *Mol. Phys.* **1982**, *46*, 651–656.
- (49) Kyte, J.; Doolittle, R. F. A Simple Method for Displaying the Hydropathic Character of a Protein. *J. Mol. Biol.* **1982**, *157*, 105–132.
- (50) Hopp, T. P.; Woods, K. R. Prediction of Protein Antigenic Determinants From Amino Acid Sequences. *Proc. Natl. Acad. Sci. U.S.A.* **1981**, *78*, 3824–3828.
- (51) Trevino, S.; Scholtz, J. M.; Pace, C. N. Amino Acid Contribution to Protein Solubility: Asp, Glu, and Ser Contribute More Favorably than the Other Hydrophilic Amino Acids in RNase Sa. *J. Mol. Biol.* **2007**, *366*, 449–460.
- (52) Katta, V.; Chait, B. T. Hydrogen/Deuterium Exchange Electrospray Ionization Mass Spectrometry: A Method for Probing Protein Conformational Changes in Solution. *J. Am. Chem. Soc.* **1993**, *115*, 6317–6321.

- (53) Kramer, R. M.; Shende, V. R.; Motl, N.; Pace, C.; Scholtz, J. Toward a Molecular Understanding of Protein Solubility: Increased Negative Surface Charge Correlates with Increased Solubility. *Biophys. J.* **2012**, *102*, 1907–1915.
- (54) Rehm, C.; Barker, J.; Bouwman, W. G.; Pynn, R. DCD USANS and SESANS: A Comparison of Two Neutron Scattering Techniques Applicable for the Study of Large-Scale Structures. *J. Appl. Crystallogr.* **2013**, *46*, 354–364.
- (55) Balu, R.; Dutta, N. K.; Choudhury, N. R.; Elvin, C. M.; Lyons, R. E.; Knott, R.; Hill, A. J. An16-Resilin: An Advanced Multi-Stimuli-Responsive Resilin-Mimetic Protein Polymer. *Acta Biomater.* **2014**, *10*, 4768–4777.
- (56) Schärtl, W. *Light Scattering from Polymer Solutions and Nanoparticle Dispersions*; Springer: Berlin, 2007.
- (57) Quiroz, F. G.; Chilkoti, A. Sequence Heuristics to Encode Phase Behaviour in Intrinsically Disordered Protein Polymers. *Nat. Mater.* **2015**, *14*, 1164–1171.
- (58) Gupta, A.; Mohanty, B.; Bohidar, H. B. Flory Temperature and Upper Critical Solution Temperature of Gelatin Solutions. *Biomacromolecules* **2005**, *6*, 1623–1627.
- (59) Li, J.; Rajagopalan, R.; Jiang, J. Role of Solvent in Protein Phase Behavior: Influence of Temperature Dependent Potential. *J. Chem. Phys.* **2008**, *128*, 235104.
- (60) Mahadevi, A. S.; Sastry, G. N. Cation- π Interaction: Its Role and Relevance in Chemistry, Biology, and Material Science. *Chem. Rev.* **2013**, *113*, 2100–2138.
- (61) Bonincontro, A.; Bultrini, E.; Calandrini, V.; Onori, G. Conformational Changes of Proteins in Aqueous Solution Induced by Temperature in the Pre-Melting Region. *Phys. Chem. Chem. Phys.* **2001**, *3*, 3811–3813.
- (62) Whittaker, J. L.; Dutta, N. K.; Knott, R.; McPhee, G.; Voelcker, N. H.; Elvin, C.; Hill, A.; Choudhury, N. R. Tunable Thermoresponsiveness of Resilin via Coassembly with Rigid Biopolymers. *Langmuir* **2015**, *31*, 8882–8891.